

# A Swarm Model for Planar Formations of Multiple Autonomous Unmanned Aerial Vehicles

Jito Vanualailai,<sup>1</sup> Ashna Sharan and Bibhya Sharma

**Abstract**—A swarm model that induces emergent collective behaviors from the individuals in the swarm is proposed for the planar formations of multiple autonomous unmanned aerial vehicles (UAVs). The stability of the formations, or cohesiveness of the swarm, is guaranteed via the the Direct Method of Lyapunov which is used to construct the instantaneous velocity of each individual. A Lyapunov-like function, from which the velocity controllers are constructed, expresses the three well-known Reynolds' flocking rules as artificial potential fields for inter-individual attraction and avoidance. Basic patterns of planar formation which are similar to emergent behaviors distinctive of swarming in nature are demonstrated via computer simulations. Different emergent patterns are obtained with variations in the system parameters.

## I. INTRODUCTION

The basic characteristics of swarming are self-organization and emergence, the absence of centralized command, the presence of distributed control and autonomy [1]. It is becoming increasingly desirable, in terms of efficiency, economy and functionality, to design multi-agent systems with similar characteristics. Hence swarming principles are being studied for their application to the design and control of multi-agent systems such as multiple planar mobile robots and multiple Unmanned Aerial Vehicles (UAVs).

Documented applications of swarming UAVs include military operations such as reconnaissance, random area search and attack, surveillance and suppression, psychological warfare, survivability enhancement, fire monitoring, data and image acquisition of targets inaccessible using ground means, localization of targets, tracking, map building, search and rescue, law enforcement, aerial mapping, traffic surveillance, inspection and cinematography. Many researchers have noted that multi-agent robotics systems designed on the principles of Swarm Intelligence [1] tend to have advantages such as (a) complex task enabling [2], [3], [4], (b) distributed sensing and action or inherent decentralization [2], (c) being more robust in case of degradation of one or some of the agents [2], [3], [5], [6], (d) scalability [6], (e) flexibility [6] and (f) having lower economic cost and ease of development compared to that involved in constructing and operating expensive single-robot systems [3].

## II. MODELING APPROACH

In 1987, Reynolds [7] proposed a set of simple rules that he believed each individual in a flock of birds instinctively followed and which led to the phenomenon of flocking:

The authors are with the School of Computing, Information & Mathematical Sciences, University of the South Pacific, Suva, Fiji.

<sup>1</sup>Corresponding author: email: jito.vanualailai@usp.ac.fj, phone: +679 323 2661; fax: +679 323 1504

- **Separation.** Each bird must steer to avoid colliding with local flockmates;
- **Alignment.** Each bird must steer towards the average heading of local flockmates;
- **Cohesion.** Each bird must steer to move towards the average position (center of mass, or centroid) of local flockmates.

In this paper, we want to solve the basic problem of navigation, or the find-path problem, for a group of autonomous aerial vehicles. However rather than proposing an algorithm that guides the UAVs to their goals, we construct control laws that incorporate the above rules from which we expect stable patterns of formation emerging. The patterns constitute the paths that the UAVs take. In other words, our principal aim is to construct control laws that uses the above swarming principles to generate stable patterns of formations for the UAVs without the requirement that the UAVs head toward any particular physical target. To meet this objective, we shall employ a method that combines both the concepts of artificial potential fields and the Direct Method of Lyapunov. The APFs ensure separation, alignment and cohesion. The functions that generate the APFs are the components of a Lyapunov-like function from which the instantaneous velocity of every member of the swarm is constructed in accordance with the Direct Method of Lyapunov to ensure the stability of the emergent pattern. Such a combined approach to swarm modeling has yield promising results in recent years, beginning with the work of Mogilner et al. [8] and Gazi and Passino [9] in 2003.

We begin by developing a simple dynamical system representing multiple rigid bodies so that it will be easily transferable to a system of quadrotor UAVs, given that UAVs are examples of rigid bodies which also require an angular coordinate to fully describe its configuration in planar space.

## III. A GENERIC 2D SWARM MODEL

Consider  $n \in \mathbb{N}$  point-like rigid bodies. The positions of the rigid bodies in 2D space can be described completely by three independent parameters, namely, two translational components and one rotational component about the vertical axis of its Body-frame reference, the yaw angle. Let the position of the  $i^{th}$  rigid body be  $(x_i, y_i) = (x_i(t), y_i(t))$  and its yaw angle be  $\psi_i = \psi_i(t)$  at time  $t \geq 0$  with initial conditions  $(x_{i0}, y_{i0}) := (x_i(t_0), y_i(t_0))$  and  $\psi_{i0} := \psi_i(t_0)$  at time  $t = t_0 \geq 0$ . If the configuration vector for the  $i^{th}$  rigid body is  $\mathbf{q}_i := (x_i, y_i, \psi_i) \in \mathbb{R}^3$ , then we can let the configuration vector for  $n$  rigid bodies be  $\mathbf{q} :=$

$(\mathbf{q}_1, \mathbf{q}_2, \mathbf{q}_3, \dots, \mathbf{q}_n) \in \mathbb{R}^{3n}$ , so that the vector that captures the initial conditions is  $\mathbf{q}_0 := \mathbf{q}(t_0)$ .

*Definition 1:* The  $i^{th}$  rigid body is the set

$$P_i := \{(z_1, z_2) \in \mathbb{R}^2 : (z_1 - x_i)^2 + (z_2 - y_i)^2 \leq r_i^2\}$$

where  $P_i$  is a disk of radius  $r_i$ .

*Definition 2:* The center of mass or *centroid* of  $n$  number of rigid bodies is defined as

$$(x_C, y_C) := \left( \frac{1}{n} \sum_{k=1}^n x_k, \frac{1}{n} \sum_{k=1}^n y_k \right).$$

Let the instantaneous velocities of the  $i^{th}$  rigid body at time  $t \geq 0$  be  $(v_{x_i}(t), v_{y_i}(t), \mu_i(t)) := (x'_i(t), y'_i(t), \psi'_i(t)) \in \mathbb{R}^3$ . Then the state space representation of our system is thus

$$\dot{\mathbf{q}} := \begin{pmatrix} \dot{\mathbf{q}}_1 \\ \vdots \\ \dot{\mathbf{q}}_n \end{pmatrix} = \begin{pmatrix} \dot{x}_1 \\ \dot{y}_1 \\ \dot{\psi}_1 \\ \vdots \\ \dot{x}_n \\ \dot{y}_n \\ \dot{\psi}_n \end{pmatrix} = \begin{pmatrix} v_{x_1} \\ v_{y_1} \\ \mu_1 \\ \vdots \\ v_{x_n} \\ v_{y_n} \\ \mu_n \end{pmatrix} =: \begin{pmatrix} f_1(\mathbf{q}) \\ f_2(\mathbf{q}) \\ f_3(\mathbf{q}) \\ \vdots \\ f_{n-2}(\mathbf{q}) \\ f_{n-1}(\mathbf{q}) \\ f_n(\mathbf{q}) \end{pmatrix} =: \mathbf{F}(\mathbf{q})$$

where  $\mathbf{F}(\mathbf{q})$  is a function assumed smooth enough to guarantee existence, uniqueness and continuous dependence of solutions of the system under consideration. In summary, our multi-agent system at time  $t \geq 0$  with initial conditions at some time  $t_0 \geq 0$  is

$$\dot{\mathbf{q}} = \mathbf{F}(\mathbf{q}), \quad \mathbf{q}_0 = \mathbf{q}(t_0). \quad (1)$$

### A. Formulation of a Lyapunov-like Function

The *agents*<sup>1</sup> are assumed to be identical hence  $r_i = r_b$  for all  $i = 1, 2, \dots, n$  where  $r_b$  is the radius of its *bin size*<sup>2</sup>.

1) *Target Convergence for Cohesion:* If we consider the centroid as the target of the  $i^{th}$  agent, then a simple function that can play the role of target convergence is

$$R_i(\mathbf{q}) := \frac{1}{2}[(x_i - x_C)^2 + (y_i - y_C)^2],$$

which resembles the Euclidean distance function between the  $i^{th}$  agent and the centroid.

2) *Yaw Angle Convergence for Alignment:* For alignment, want all the yaw angles to eventually converge to a common value. Thus we propose the function

$$A_{ij}(\mathbf{q}) := \frac{1}{2}(\psi_i - \psi_j)^2, \quad \forall j \neq i.$$

<sup>1</sup>Henceforth ‘‘agent’’ will be used to refer to the units of a swarm whether it is a swarm of rigid bodies or UAVs.

<sup>2</sup>Bin size is the area enclosed by the closed circular curve drawn around agents, marking the region as the boundary inside which it is safe from collision.

3) *Obstacle Avoidance for Separation:* For separation between the  $i^{th}$  and the  $j$ th agents, it is natural to define the Euclidean distance function

$$Q_{ij}(\mathbf{q}) := \sqrt{(x_i - x_j)^2 + (y_i - y_j)^2} - 2r_b, \quad \forall j \neq i.$$

The physical limitation that no two agents can occupy the same space at the same time requires us to impose the condition that

$$\sqrt{(x_i - x_j)^2 + (y_i - y_j)^2} > 2r_b, \quad \forall j \neq i. \quad (2)$$

### B. A Tentative Lyapunov-like Function

Introduce  $\gamma_i > 0$ ,  $\varepsilon_{ij} > 0$  and  $\beta_{ij} > 0$  as cohesion, convergence and collision avoidance parameters, respectively. Then a tentative Lyapunov-like function for system (1) is

$$L = L(\mathbf{q}) := \sum_{i=1}^n R_i[\gamma_i + \sum_{\substack{j=1 \\ j \neq i}}^n (\frac{\beta_{ij}}{Q_{ij}} + \varepsilon_{ij} A_{ij})]. \quad (3)$$

The domain over which  $L > 0$  is defined as

$$D_1(L) := \{\mathbf{q} \in \mathbb{R}^{3n} : Q_{ij}(\mathbf{q}) > 0, \forall j \neq i\}$$

to reflect condition (2). Now, the time-derivative of the tentative Lyapunov-like function along a trajectory of system (1) is

$$\begin{aligned} \dot{L}_{(1)} = & \sum_{i=1}^n \left\{ (x_i - x_C)[\gamma_i + \sum_{\substack{j=1 \\ j \neq i}}^n (\varepsilon_{ij} A_{ij} + \frac{\beta_{ij}}{Q_{ij}})] \right. \\ & \left. - 2R_i \sum_{\substack{j=1 \\ j \neq i}}^n \frac{\beta_{ij}(x_i - x_j)}{(Q_{ij})^2(Q_{ij} + 2r_b)} \right\} \dot{x}_i \\ & + \sum_{i=1}^n \left\{ (y_i - y_C)[\gamma_i + \sum_{\substack{j=1 \\ j \neq i}}^n (\varepsilon_{ij} A_{ij} + \frac{\beta_{ij}}{Q_{ij}})] \right. \\ & \left. - 2R_i \sum_{\substack{j=1 \\ j \neq i}}^n \frac{\beta_{ij}(y_i - y_j)}{(Q_{ij})^2(Q_{ij} + 2r_b)} \right\} \dot{y}_i \\ & + \sum_{i=1}^n \left\{ 2R_i \sum_{\substack{j=1 \\ j \neq i}}^n (\psi_i - \psi_j) \right\} \dot{\psi}_i, \end{aligned}$$

from which we get the following entries of the gradient of  $L$ :

$$\begin{aligned} \frac{\partial L}{\partial x_i} &= (x_i - \frac{1}{n} \sum_{k=1}^n x_k) [\gamma_i + \sum_{\substack{j=1 \\ j \neq i}}^n (\varepsilon_{ij} A_{ij} + \frac{\beta_{ij}}{Q_{ij}})] \\ &\quad - 2R_i \sum_{\substack{j=1 \\ j \neq i}}^n \frac{\beta_{ij}(x_i - x_j)}{(Q_{ij})^2(Q_{ij} + 2r_b)}, \end{aligned} \quad (4a)$$

$$\begin{aligned} \frac{\partial L}{\partial y_i} &= (y_i - \frac{1}{n} \sum_{k=1}^n y_k) [\gamma_i + \sum_{\substack{j=1 \\ j \neq i}}^n (\varepsilon_{ij} A_{ij} + \frac{\beta_{ij}}{Q_{ij}})] \\ &\quad - 2R_i \sum_{\substack{j=1 \\ j \neq i}}^n \frac{\beta_{ij}(y_i - y_j)}{(Q_{ij})^2(Q_{ij} + 2r_b)}, \end{aligned} \quad (4b)$$

$$\frac{\partial L}{\partial \psi_i} = 2R_i \sum_{\substack{j=1 \\ j \neq i}}^n (\psi_i - \psi_j). \quad (4c)$$

Hence,

$$\begin{aligned} \dot{L}_{(1)} &= \sum_{i=1}^n [\frac{\partial L}{\partial x_i} \dot{x}_i + \frac{\partial L}{\partial y_i} \dot{y}_i + \frac{\partial L}{\partial \psi_i} \dot{\psi}_i] \\ &= \sum_{i=1}^n [\frac{\partial L}{\partial x_i} \nu_{xi} + \frac{\partial L}{\partial y_i} \nu_{yi} + \frac{\partial L}{\partial \psi_i} \mu_i]. \end{aligned} \quad (5)$$

### C. Velocity Controllers

Let  $\delta_i, \kappa_i, \sigma_i > 0$  be real numbers. If we let the velocity controllers be such that

$$\nu_{xi} := -\delta_i \frac{\partial L}{\partial x_i}, \quad \nu_{yi} := -\kappa_i \frac{\partial L}{\partial y_i} \quad \text{and} \quad \mu_i := -\sigma_i \frac{\partial L}{\partial \psi_i}, \quad (6)$$

then we easily have

$$\dot{L}_{(1)} = - \sum_{i=1}^n [\frac{\nu_{xi}^2}{\delta_i} + \frac{\nu_{yi}^2}{\kappa_i} + \frac{\mu_i^2}{\sigma_i}] \leq 0. \quad (7)$$

### D. Stability Analysis

First we identify the equilibrium points of system (1).

*Lemma 1:* If the set  $E = \{\mathbf{q} \in D_1(L) : \dot{L}_{(1)}(\mathbf{q}) = 0\}$  is non-empty, then it is a set of equilibrium points  $\mathbf{q}_e$  of system (1).

*Proof:* From equations (5)–(7), it is clear that  $\dot{L}_{(1)}(\mathbf{q}) = 0$  and  $\dot{\mathbf{q}} = \mathbf{0}$  if and only if

$$\frac{\partial L}{\partial x_i} = \frac{\partial L}{\partial y_i} = \frac{\partial L}{\partial \psi_i} = 0. \quad \blacksquare$$

It is now straightforward to use LaSalle's Invariance Principle to determine the behavior of system (1) in the vicinity of  $E$ . Following Gazi and Passino [9], we prove the following result.

*Theorem 1:* Let  $E$  be non-empty. Then  $\mathbf{q}(t) \rightarrow E$  as  $t \rightarrow \infty$ .

*Proof:* If  $E$  is non-empty, then it is an invariant set of equilibrium points of (1) by Lemma 1. Thus, by LaSalle's

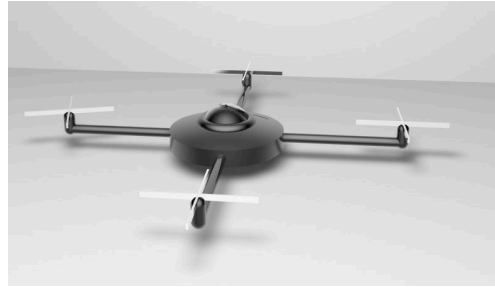


Fig. 1. A drawing of a quadrotor. Copyright granted by Shutterstock, www.shutterstock.com.

Invariance Principle, as  $t \rightarrow \infty$ , the state  $\mathbf{q}$  converges to the largest invariant subset of  $E$ .  $\blacksquare$

We have thus successfully constructed a Lyapunov-like function that guarantees there will be a constant arrangement about a stationary centroid if system (1) has equilibrium points in  $D_1(L)$ . Of course if  $E$  is empty, then the centroid is non-stationary. In this situation, the solutions are bounded with respect to the moving centroid since  $L > 0$  and  $\dot{L}_{(1)} \leq 0$  in  $D_1(L)$ .

## IV. APPLICATION TO MULTIPLE QUADROTOR UAVS

The specific type of UAVs being considered in this paper is the miniature sized quadrotor helicopter-type.<sup>3</sup> Shown in Figure 1 is an example of a quadrotor UAV design. Without any particular “nose” or “tail” synonymous with the non-holonomic airplane, there is some flexibility in developing a kinematic model. In order to apply our methodology, we treat the kinematic model of the quadrotor UAVs as a 2D geometric problem, noting that such 2D representations have been made by other researchers using mainly the uni-cycle model [10]. Figure 2 shows the configuration space for  $n = 3$  UAVs from a bird's-eye view.

In 2D planar space, the altitude and the pitch and roll angles are not considered as variables. The axis along which the quadrotor moves back and forth is denoted the longitudinal axis and its perpendicular counterpart along which it moves sideways the lateral axis. The longitudinal and lateral axes can be considered a transformation (rotation of  $\psi$  degrees) of the Body-frame reference about  $z_B$ . Hence the  $i^{th}$  UAV is centered at  $(x_i, y_i)$ , with yaw angle  $\psi_i$ . With respect to the Earth-frame reference it also has an orientation  $\theta_i$  which describes its orientation with respect to the line of motion. The linear velocities are denoted by  $\nu_{xi}$  and  $\nu_{yi}$  along the longitudinal and lateral axes respectively while the rotational velocities are denoted by  $\mu_i$  (time derivative of  $\psi_i$ ) and  $\omega_i$  (time-derivative of  $\theta_i$ ). Hence, the configuration of the  $i^{th}$  quadrotor UAV is given as  $(x_i, y_i, \psi_i, \theta_i) \in \mathbb{R}^4$  as shown in Figure 3. The bin size of the quadrotor UAV is taken as  $r_b$  while the length of its arms is denoted by  $\ell$  whereby  $\ell \leq r_b$ . By controlling the difference between  $\ell$  and  $r_b$  the spacing in between the agents can be controlled as they converge to

<sup>3</sup>Quadrotor UAVs are helicopter-type in the sense they exhibit vertical take off and landing.

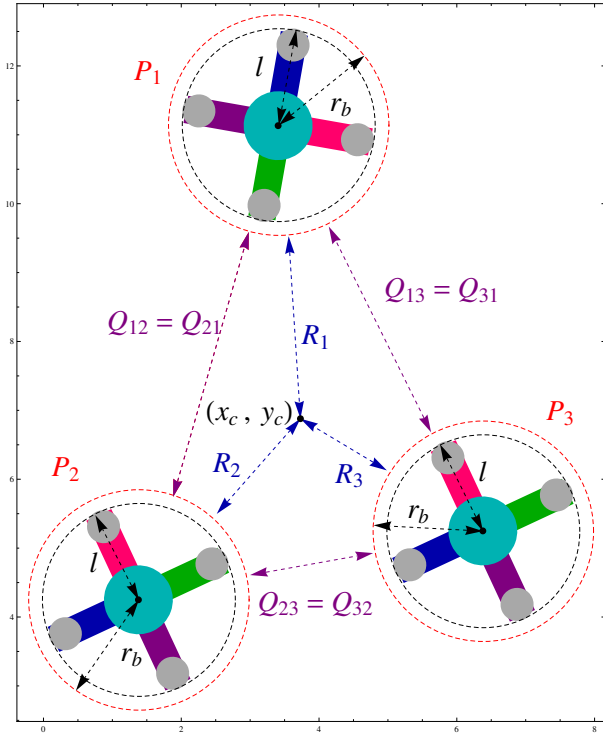


Fig. 2. A bird's-eye view of 3 quadrotor UAVs.

the centroid and move cohesively. This will be demonstrated with simulations in the next section.

With reference to Figure 3 we see that for a rotor (of some  $i_{th}$  quadrotor UAV) that falls on the line of motion of linear velocity  $\nu_i$ , the velocity components can be defined as

$$\left. \begin{aligned} \dot{x}_{1i} &:= \nu_{x_i} \cos \psi_i - \nu_{y_i} \sin \psi_i, \\ \dot{y}_{1i} &:= \nu_{x_i} \sin \psi_i + \nu_{y_i} \cos \psi_i. \end{aligned} \right\} \quad (8)$$

We also see that a rotor located directly opposite the first one at  $(x_{2i}, y_{2i})$  is related to it by

$$x_{2i} = x_{1i} + 2l \cos \theta_i \text{ and } y_{2i} = y_{1i} + 2l \sin \theta_i,$$

where  $2l$  is the distance between two oppositely located rotors. From these, we get

$$\dot{x}_{2i} = \dot{x}_{1i} - 2l\dot{\theta}_i \sin \theta_i \text{ and } \dot{y}_{2i} = \dot{y}_{1i} + 2l\dot{\theta}_i \cos \theta_i. \quad (9)$$

The center of the UAV, given by  $(x_i, y_i)$ , is the midpoint of the two oppositely located rotors, where

$$x_i = \frac{1}{2}(x_{1i} + x_{2i}) \text{ and } y_i = \frac{1}{2}(y_{1i} + y_{2i}), \quad (10)$$

from which

$$\dot{x}_i = \frac{1}{2}(\dot{x}_{1i} + \dot{x}_{2i}) \text{ and } \dot{y}_i = \frac{1}{2}(\dot{y}_{1i} + \dot{y}_{2i}).$$

Substituting (8) and (9) into them, we get the velocities with respect to the center of the UAV:

$$\left. \begin{aligned} \dot{x}_i &= \nu_{x_i} \cos \psi_i - \nu_{y_i} \sin \psi_i - l\dot{\theta}_i \sin \theta_i, \\ \dot{y}_i &= \nu_{x_i} \sin \psi_i + \nu_{y_i} \cos \psi_i + l\dot{\theta}_i \cos \theta_i. \end{aligned} \right.$$

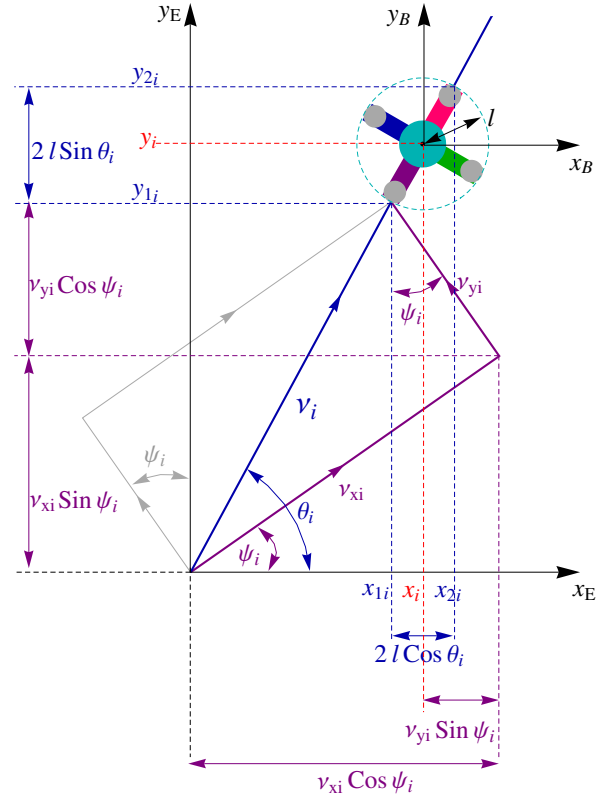


Fig. 3. Kinematic Model of a Quadrotor UAV.

Hence the kinematic model of the  $i_{th}$  UAV is given by

$$\left. \begin{aligned} \dot{x}_i &= \nu_{x_i} \cos \psi_i - \nu_{y_i} \sin \psi_i - l\omega_i \sin \theta_i \\ \dot{y}_i &= \nu_{x_i} \sin \psi_i + \nu_{y_i} \cos \psi_i + l\omega_i \cos \theta_i \\ \dot{\psi}_i &= \mu_i \\ \dot{\theta}_i &= \omega_i \end{aligned} \right\} \quad (11)$$

where  $(x_i, y_i)$  is its center and  $\mu_i$  represents the angular velocity of the quadrotor UAV as it turns on its vertical axis, that is,  $(z_B)$  of the Body-frame reference  $(x_B, y_B, z_B)$ . This motion is called “yawing”, which is instantaneous rate of change of the yaw angle,  $\psi_i$ , with respect to time, while  $\omega_i$  represents the angular velocity of the UAV with respect to its Earth-frame reference  $(x_E, y_E, z_E)$ .

Now, if we let  $\mathbf{p}_i := (x_i, y_i, \psi_i, \theta_i) \in \mathbb{R}^4$  and  $\mathbf{p} := (\mathbf{p}_1, \dots, \mathbf{p}_n) \in \mathbb{R}^{4n}$ , then we can capture (11) via

$$\dot{\mathbf{p}} =: \mathbf{G}(\mathbf{p}), \quad \mathbf{p}_0 = \mathbf{p}(t_0), \quad t_0 \geq 0, \quad (12)$$

where  $\mathbf{G}$  is a  $4n \times 1$  vector with entries consisting of righthand terms in (11) for  $i = 1, \dots, n$ .

The Lyapunov-like function for (12) is the same as (3), but with the independent variable  $\mathbf{p}$  rather than  $\mathbf{q}$ , and with the new domain  $D_2(L) := \{\mathbf{p} \in \mathbb{R}^{4n} : Q_{ij}(\mathbf{p}) > 0\}, \forall j \neq i$ .

Along a solution of system (12), we get

$$\begin{aligned}
\dot{L}_{(12)} &= \sum_{i=1}^n \left[ \dot{x}_i \frac{\partial L}{\partial x_i} + \dot{y}_i \frac{\partial L}{\partial y_i} + \dot{\psi}_i \frac{\partial L}{\partial \psi_i} \right] \\
&= \sum_{i=1}^n \left[ (\nu_{x_i} \cos \psi_i - \nu_{y_i} \sin \psi_i - \ell \dot{\theta}_i \sin \theta_i) \frac{\partial L}{\partial x_i} \right. \\
&\quad \left. + (\nu_{x_i} \sin \psi_i + \nu_{y_i} \cos \psi_i + \ell \dot{\theta}_i \cos \theta_i) \frac{\partial L}{\partial y_i} + \mu_i \frac{\partial L}{\partial \psi_i} \right] \\
&= \sum_{i=1}^n \left[ \left( \frac{\partial L}{\partial x_i} \cos \psi_i + \frac{\partial L}{\partial y_i} \sin \psi_i \right) \nu_{x_i} \right. \\
&\quad \left. + \left( \frac{\partial L}{\partial y_i} \cos \psi_i - \frac{\partial L}{\partial x_i} \sin \psi_i \right) \nu_{y_i} \right. \\
&\quad \left. + \left( -\frac{\partial L}{\partial x_i} \ell \sin \theta_i + \frac{\partial L}{\partial y_i} \ell \cos \theta_i \right) \omega_i + \frac{\partial L}{\partial \psi_i} \mu_i \right],
\end{aligned}$$

where  $\partial L/\partial x_i$ ,  $\partial L/\partial y_i$  and  $\partial L/\partial \psi_i$  are defined by equations (4a), (4b), and (4c), respectively. Now, let  $\delta_i, \kappa_i, \sigma_i, \rho_i > 0$  be real constants and

$$\nu_{x_i} := -\delta_i \left( \frac{\partial L}{\partial x_i} \cos \psi_i + \frac{\partial L}{\partial y_i} \sin \psi_i \right), \quad (13a)$$

$$\nu_{y_i} := -\kappa_i \left( -\frac{\partial L}{\partial x_i} \sin \psi_i + \frac{\partial L}{\partial y_i} \cos \psi_i \right), \quad (13b)$$

$$\omega_i := -\rho_i \left( -\frac{\partial L}{\partial x_i} \ell \sin \theta_i + \frac{\partial L}{\partial y_i} \ell \cos \theta_i \right), \quad (13c)$$

$$\mu_i := -\sigma_i \frac{\partial L}{\partial \psi_i}. \quad (13d)$$

Then we have

$$\dot{L} = - \sum_{i=1}^n \left[ \frac{\nu_{x_i}^2}{\delta_i} + \frac{\nu_{y_i}^2}{\kappa_i} + \frac{\omega_i^2}{\rho_i} + \frac{\mu_i^2}{\sigma_i} \right] \leq 0.$$

Equations (13a)-(13d) thus constitute our velocity controllers for system (12).

## V. SIMULATION RESULTS

Parameters and initial configurations are randomized in our algorithms in order to obtain different patterns of formation by trial and error. The initial configuration are observed to play just as significant a role as the parameters in determining the type of pattern that emerges. The Lyapunov-like function dictates that the yaw angles  $\psi_i$  converge to a singular constant value, which implies that UAVs' yawing motion eventually becomes zero irrespective of the emergent pattern. On the other hand, the orientation with respect to the Earth-frame reference and its rate of change given by  $\omega_i$  determines the emergent pattern of formation. We observed that if  $\omega_i = 0$  for all agents then the pattern that results was either a constant arrangement about the centroid or a parallel formation. If  $\omega_i \neq 0$  and were the same for all agents, then a stable circular formation resulted; however, different values of  $\omega_i \neq 0$  yielded stable oscillatory patterns. In the simulations shown in Figure 4 to Figure 6, the trajectories of the UAVs are shown in thin lines and the trajectory of the centroid is shown as a thick line.

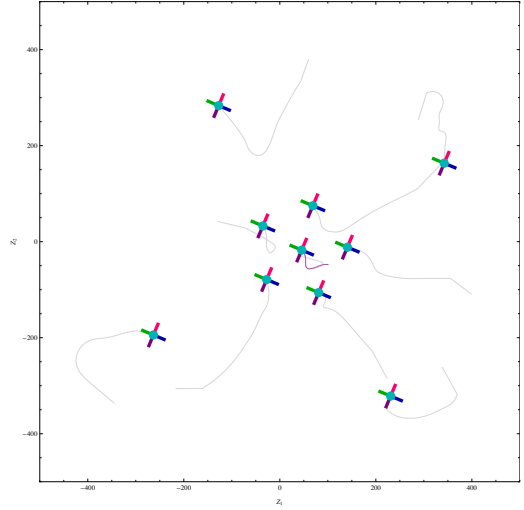


Fig. 4. **Hover Arrangement about a Stationary Centroid.** There are  $n = 10$  quadrotor UAVs in a stationary or hover formation at time  $t=308$  with bin size  $r_b = 25$  and  $\ell = 24$ . The thick line shows the trajectory of the centroid. The parameters are  $\delta_i = 1, \kappa_i = 1, \sigma_i = 1, \rho_i = 1, \varepsilon_i = 1, \gamma_i = .01$  and  $\beta_{ij} = 5$ .

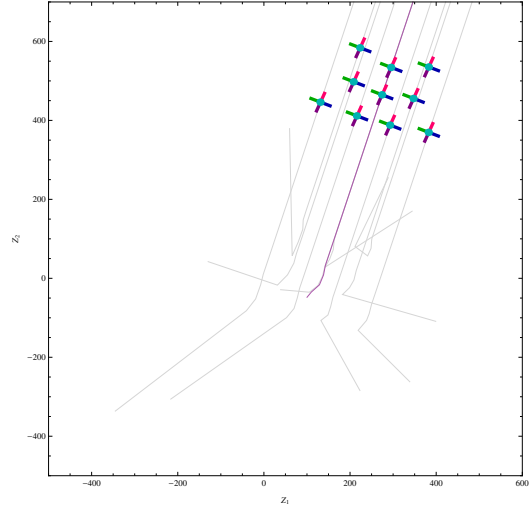


Fig. 5. **Parallel Formation.** In this scenario, the initial positions and orientations, and the parameters are kept the same as those used in the scenario shown in Figure 4, but with  $\gamma_i = 2$  and  $\beta_{ij} = 10$ .

For the case  $\psi_i = \theta_i$ , system (11) is car-like, with

$$\begin{aligned}
\dot{x}_i &= \nu_{x_i} \cos \theta_i - \nu_{y_i} \sin \theta_i - \ell \omega_i \sin \theta_i, \\
\dot{y}_i &= \nu_{x_i} \sin \theta_i + \nu_{y_i} \cos \theta_i + \ell \omega_i \cos \theta_i, \quad \dot{\theta}_i = \omega_i,
\end{aligned}$$

and

$$\begin{aligned}
\nu_{x_i} &= -\delta_i \left( \frac{\partial L}{\partial x_i} \cos \theta_i + \frac{\partial L}{\partial y_i} \sin \theta_i \right), \\
\nu_{y_i} &= -\kappa_i \left( -\frac{\partial L}{\partial x_i} \sin \theta_i + \frac{\partial L}{\partial y_i} \cos \theta_i \right), \\
\omega_i &= -\rho_i \left( -\frac{\partial L}{\partial x_i} \ell \sin \theta_i + \frac{\partial L}{\partial y_i} \ell \cos \theta_i + \frac{\partial L}{\partial \theta_i} \right).
\end{aligned}$$

In this instance, when (12) is simulated, there is a major difference seen in the behavior of the quadrotor UAVs. It

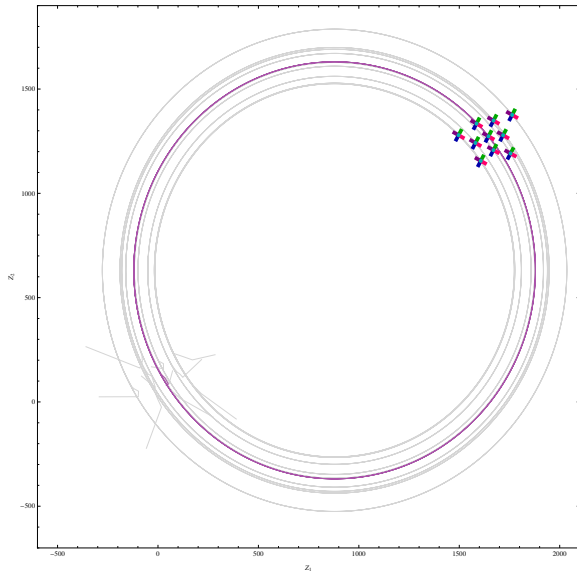


Fig. 6. **Stable Circular Formation.** Here,  $\ell = 24$ ,  $r_b = 35$ ,  $\delta_i = 1$ ,  $\kappa_i = 1$ ,  $\sigma_i = 1$ ,  $\rho_i = 1$ ,  $\varepsilon_i = 1$  and  $\gamma_i = 1$ , whilst  $\beta_{ij}$  were randomized between 1 and 10. The UAVs are moving in the anti-clockwise direction.

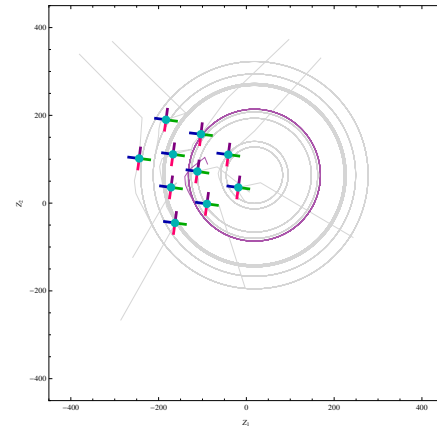
now shows car-like motion as demonstrated in Figure 7 as if it has a distinct front and rear with non-holonomic constraints so that it can not move sideways and must steer. In this case the yaw angle is equal to the angle with respect to Earth-frame reference which is nonzero hence angular motion is observed with respect to both frames of reference, the Earth-frame and the quadrotors' Body-frame.

## VI. CONCLUSION AND FURTHER WORK

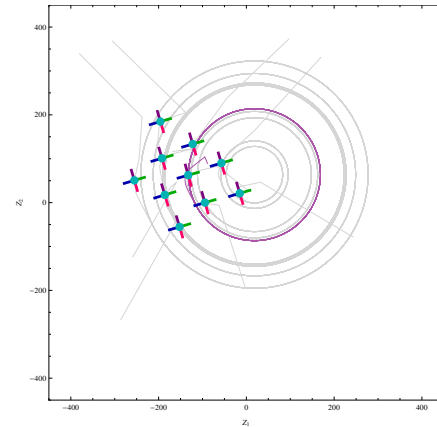
The computer aided swarm modeling process tests the Lyapunov-like functions and subsequent velocity control laws constructed, demonstrating the desired outcome of convergence to the centroid, lasting cohesion of the swarm as a whole and collision avoidance amongst the swarm agents. The resultant emergent behaviors of our swarming UAVs were stationary arrangement about the centroid, parallel formations, and stable oscillatory formations. The simplicity of the control algorithms is an advantage of our swarm model. However it is a model with a bird's-eye view and which has scope for development in directions such as the inclusion of altitude and Euler angles (roll, pitch) as variables to model the complete dynamics of such quadrotor UAVs in the three-dimensional state-space with and without the presence of static obstacles. In addition, a system of UAVs is a mechanical system; hence, any model representing such a system must account for physical limitations on the velocities. The swarm model in this paper lacks such velocity constraints and has room for improvement in this aspect as well.

## REFERENCES

[1] E. Bonebeau, M. Dorigo, and G. Theraulaz, *Swarm Intelligence: From Natural to Artificial Systems*. New York: Oxford University Press, 1999.



(a) Positions at  $t = 3$ .



(b) Positions at  $t = 4$

Fig. 7. **Car-like Behavior.** Positions and orientations of  $n = 10$  UAVs showing a change in the yaw angles of the UAVs.

[2] A. Martinoli, *Swarm Intelligence in Autonomous Collective Robotics: From Tools to the Analysis and Synthesis of Distributed Control Strategies*. PhD, Polytechnique Federale de Lausanne, 1999.

[3] J. Liu and J. Wu, *Multi-Agent Robotic Systems*, vol. 21 of *International Series on Computational Intelligence*. The CRC Press, 2001.

[4] M. Hsieh, A. Cowley, A. Keller, J. Chaimowicz, B. Grocholsky, V. Kumar, C. J. Taylor, Y. Endo, R. C. Arkin, and B. Jung, "Adaptive teams of autonomous aerial and ground robots for situational awareness," *Journal of Field Robotics*, vol. 24, no. 11-12, pp. 991-1014, 2007.

[5] L. Chaimowicz and V. Kumar, "Aerial shepherds: Coordination among uavs and swarms of robots," *Distributed Autonomous Robotic Systems 6*, pp. 243-252, 2007.

[6] J. Bennet, Derek, C. R. McInnes, M. Suzuki, and K. Uchiyama, "Autonomous three-dimensional formation flight for a swarm of unmanned aerial vehicles," *Journal of Guidance, Control and Dynamics*, vol. 34, pp. 1899-1908, Dec. 2011.

[7] C. W. Reynolds, "Flocks, herds, and schools: A distributed behavioral model, in computer graphics," in *Procs. of the 14th annual conference on Computer graphics and interactive techniques*, (New York, USA), pp. 25-34, 1987.

[8] A. Mogilner, L. Edelstein-Keshet, L. Bent, and A. Spiros, "Mutual interactions, potentials, and individual distance in a social aggregation," *Journal of Mathematical Biology*, vol. 47, pp. 353-389, 2003.

[9] V. Gazi and K. Passino, "Stability analysis of swarms," *IEEE Transactions on Automatic Control*, vol. 48, pp. 692-697, 2003.

[10] F. Morbidi, R. A. Freeman, and K. M. Lynch, "Estimation and control of UAV swarms for distributed monitoring tasks," in *American Control Conference*, (San Francisco, CA), June 2011.